Electron spectroscopy of europium

1990 J. Phys.: Condens. Matter 2 3643

(http://iopscience.iop.org/0953-8984/2/15/019)

J. Phys.: Condens. Matter **2** (1990) 3643–3658. Printed in the UK

Electron spectroscopy of europium

W H Hocking† and J A D Matthew‡

† Atomic Energy of Canada Limited, Whiteshell Nuclear Research Establishment, Pinawa, Manitoba R0E 1L0, Canada

‡ Department of Physics, University of York, Heslington, York YO1 5DD, UK

Received 24 October 1989

Abstract. Electron emission spectra of Eu, $EuAl_2$ and Eu_2O_3 arising from excitation of the europium 4d subshell by 0.5–5 keV electron impact and Al Kα x-radiation have been compared. The electron-impact-excited emission structure has been assigned primarily to the $N_{45}O_{23}O_{23}$, $N_{45}O_{23}N_{67}$ and $N_{45}N_{67}N_{67}$ normal Auger transitions and the 4f(4d ← 4f) direct recombination process; Auger transitions with a $\overline{4, \varepsilon f}$ spectator electron and the 5p(4d ← 4f) direct recombination process appear to be of secondary importance. Europium 4d → 4f giant resonance excitation has been monitored by electron energy loss spectroscopy and correlated with the direct recombination features. The electron emission excited by Al Kα x-radiation has been shown to be predominantly due to Auger transitions with a spectator vacancy: $N_{45}N$–$NO_{23}O_{23}$, $N_{45}N$–$NO_{23}N_{67}$ and $N_{45}N$–$NN_{67}N_{67}$. Argon-ion bombardment of europium has been found to excite normal 4d-based Auger electron emission but not direct recombination electron emission.

1. Introduction

The electron emission spectra of the rare earths arising from excitation of the 4d subshell by electron impact have been extensively analysed [1–10]. A complex emission structure is observed in the kinetic energy range 60–190 eV, which for the lighter rare earths can be described as a quartet of partly overlapped peaks. The first three of these peaks, in ascending order by energy, have been attributed primarily to the Auger transitions $N_{45}O_{23}O_{23}$, $N_{45}O_{23}N_{67}$ and $N_{45}N_{67}N_{67}$. There is, however, probably some contribution to the electron emission intensity in this region from 4d-based Auger transitions involving valence (6s and 5d) and O_1 electrons. For the heavier rare earths, spin–orbit splitting and multiplet structure broaden the emission into a wide band with less well defined features. Further complexity may be introduced by Auger transitions arising from ionisation of the 4p subshell, $N_{23}N_{45}N_{67}$ and $N_{23}N_{45}O_{23}$, which should overlap the 4d-based electron emission and might have significant intensity [1, 6].

Dufour and Bonnelle [9] first identified the highest-energy feature in the 4d-based electron emission structure excited from the rare earths by electron impact as a direct recombination transition of the type $[Kr]4d^95s^25p^64f^nV^{n*}\,\overline{4, \varepsilon f}^1 \rightarrow [Kr]4d^{10}5s^25p^64f^{n-1}V^{n*} + e$. The $[Kr]4d^95s^25p^64f^nV^{n*}\,\overline{4, \varepsilon f}^1$ excited state is populated by a giant resonance transition, $[Kr]4d^{10}5s^25p^64f^nV^{n*} \rightarrow [Kr]4d^95s^25p^64f^nV^{n*}\,\overline{4, \varepsilon f}^1$, in which a 4d electron is promoted into a hybrid $l = 3$ state with both localised (nf) and continuum (εf) character [11–17]. Because of the large 4d–

0953-8984/90/153643 + 16 $03.50

4f exchange interaction, the strongest multiplet components of the giant resonance transition occur at energies well above the 4d ionisation threshold [18], except for the heaviest rare earths. Since the $4f^{n-1}$ final state is also less excited than the $4f^{n-2}$ final state, the primary 4f(4d ← 4f) direct recombination emission may occur at upwards of 10 eV higher kinetic energy than the $N_{45}N_{67}N_{67}$ Auger electron transition [1–4, 8, 9, 18]. Alternative decay channels from the $[Kr]4d^9 5s^2 5p^6 4f^n V^{n^*} \overline{4, \varepsilon f}^1$ excited state include autoionisation followed by conventional Auger transitions and direct recombination processes involving valence, 5p or 5s electrons [18]. For the light rare earths, the 5p(4d ← 4f) direct recombination process, $[Kr]4d^9 5s^2 5p^6 4f^n V^{n^*} \overline{4, \varepsilon f}^1 \rightarrow [Kr]4d^{10} 5s^2 5p^5 4f^n V^{n^*} + e$, contributes substantial intensity to the third peak in the quartet of electron emission features, which is normally identified with the $N_{45}N_{67}N_{67}$ Auger transition [1].

The $[Kr]4d^{10} 5s^2 5p^6 4f^n V^{n^*} \rightarrow [Kr]4d^9 5s^2 5p^6 4f^n V^{n^*} \overline{4, \varepsilon f}^1$ giant resonance excitation has been systematically investigated by synchrotron x-ray spectroscopy [12, 14, 16, 17, 19–33] and electron energy loss spectroscopy (EELS) [34–40]. Recently, Richter *et al* [41] have studied the electron emission spectra of the rare-earth vapours, where the Auger and direct recombination features are more clearly separated owing to the absence of extra-atomic relaxation. The existence of alternative decay channels from the $[Kr]4d^9 5s^2 5p^6 4f^n V^{n^*} \overline{4, \varepsilon f}^1$ excited state has also been demonstrated by photoion spectroscopy [42]; interpretation was based upon atomic partial photoionisation cross sections calculated using the time-dependent local-density approximation [43]. Spin-polarised electron emission spectroscopy on gadolinium has provided additional support for the above picture [44]. The nature of giant resonances has been comprehensively reviewed by Connerade *et al* [45].

The $[Kr]4d^9 5s^2 5p^6 4f^n V^{n^*} \overline{4, \varepsilon f}^1$ excited state can be populated by electron impact for any primary electron energy E_p greater than the giant resonance transition energy E_{GR}, since an impinging electron can lose a fraction of its kinetic energy. Conversely, this excited state is accessible by x-ray absorption only if the photon energy is exactly at resonance, $h\nu = E_{GR}$. It should therefore be feasible to distinguish between Auger and direct recombination features in the electron emission spectra of the rare earths by comparing electron-impact excitation with non-resonant x-ray excitation. Although (non-resonant) characteristic x-radiation cannot excite the giant resonance transition directly, some excitation might occur indirectly by bremsstrahlung radiation or by high-energy electrons (Auger electrons or photoelectrons) generated at the surface. Dufour *et al* [8] and Netzer *et al* [2] have compared electron-impact excitation with x-ray excitation (Al or Mg Kα) for metallic samarium and erbium, respectively. In both cases, despite problems with background subtraction, the electron-impact-excited emission was clearly shown to have substantial additional intensity on the high-kinetic-energy side—consistent with the direct recombination, following giant resonance excitation, assignment. Subtle additional differences were also observed, however, between the emission structures for the two excitation modes.

The electron emission arising from excitation of the 4d subshell of europium has been investigated in further detail. This work was prompted by the peculiar spectra observed during a scanning Auger microscopy study of europium partitioning in sphene ($CaTiSiO_5$) glass ceramics [46]. Electron emission has been excited from elemental europium, europium aluminide ($EuAl_2$) and europium sesquioxide (Eu_2O_3) by 0.5–5 keV electron impact and Al Kα x-radiation. For each of these materials, the europium 4d → 4f giant resonance excitation has also been measured by EELS and correlated with the resulting direct recombination processes. In addition, 4d-based electron emission has been excited from Eu metal by argon-ion bombardment.

2. Experimental procedures

The electron emission spectra excited by electron impact and argon-ion bombardment were recorded on a computer(DEC PDP 11/34)-controlled SAM 590A scanning Auger microscope manufactured by the Physical Electronics Division (PHI) of Perkin–Elmer Corporation. Electron energy loss studies were performed in reflection geometry on the same instrument. The SAM 590A is equipped with a 10 kV electron gun coaxially mounted in a single-pass cylindrical mirror analyser (CMA) and a 5 kV differentially pumped inert-gas ion gun. The spectrometer kinetic energy scale was calibrated using copper, silver and tantalum standards [47]. A base pressure of 5×10^{-8} Pa or lower was maintained in the system vacuum chamber by a combination of sputter-ion and titanium-sublimation pumping. Electron-impact-excited spectra were recorded using 2–5 nA of primary electron current focused into a beam with a diameter of about 0.5–1 μm at an accelerating potential of 0.5–5 kV. The electron beam was incident on the sample at an angle of 60° to the mean surface normal; it was rastered over a relatively large area (30 μm × 60 μm or more), as appropriate, to minimise charging and electron damage effects. Ion-bombardment excitation was achieved using about 150 nA of Ar^+ current in a fixed 4.5 keV beam with a diameter of about 200 μm. The Ar^+ beam was incident on the sample at an angle of 33° to the surface normal. All electron kinetic energy data were collected in the pulse-counting, or $N(E)E$, mode, with an analyser resolution $\Delta E/E$ of 0.3% (0.6% for survey spectra).

The x-ray-excited electron emission spectra were recorded on a computer(DEC 11/24)-controlled PHI SAM/ESCA 570 instrument, which is equipped with a double-pass cylindrical mirror analyser. Aluminium Kα x-rays were incident on the sample at an angle of 50° to the mean surface normal and at an angle of 90° to the CMA axis. Data were collected in the pulse-counting format, with the kinetic energy analyser operated in the non-retardation mode at a resolution of 0.3%. The non-retardation mode, $N(E)E$, was selected for this study instead of the more conventional retardation mode, $N(E)/E$, to minimise the steeply rising background at low kinetic energy (50–150 eV range of interest) and to facilitate comparison with the electron-impact-excited results.

Polycrystalline europium metal foil (0.25 mm thick) and europium sesquioxide powder were purchased from Alfa Products (Thiokol/Ventron Division). Europium aluminide, in the form of coarse grains (1 mm or less), was purchased from Cerac Inc. The Eu and $EuAl_2$ were supplied in sealed containers under argon and were transferred into the vacuum chambers without exposure to the atmosphere. Europium metal foil specimens were firmly attached (with screws) to stainless steel sample-transfer mounts. For x-ray excited electron emission studies, Eu_2O_3 and $EuAl_2$ were deposited as thin layers on segments of copper-backed adhesive tape. Prevention of extreme and unstable sample-charging conditions during electron-impact excitation of Eu_2O_3 and $EuAl_2$ was achieved by embedding grains of material in gold films sputtered onto the adhesive layer of copper tape.

A variety of procedures were employed for surface cleaning prior to analysis. Europium metal foil specimens were initially either abraded with a file in a glove box (for x-ray studies) or heavily argon-ion sputter etched (for electron-impact and ion-impact studies) to remove the surface oxide layer. A thinner oxide film on $EuAl_2$ was penetrated with moderate ion-sputter etching, whereas only light ion-sputter etching was required to remove surface contamination from Eu_2O_3. Further ion-sputter etching was performed before recording each spectrum from Eu and $EuAl_2$.

The positions of electron emission features were measured on seven-point smoothed spectra displayed in the $N(E)E$ format. The electron kinetic energy was referenced to

the vacuum level with a spectrometer work function of 4.3 eV. Surface charging was measured using known transitions and corrections applied as required. All the x-ray-excited electron emission spectra were charge calibrated using the Eu $3d_{5/2}$ XPS peak. The kinetic energy of this peak was taken to be 356.5 eV for Eu and $EuAl_2$ (binding energy, 1125.8 eV) [48–50] and 346.9 eV for Eu_2O_3 (binding energy, 1135.4 eV) [50], yielding surface charge values of 0.0 eV, +1.0 eV and +(3–4) eV, respectively. In the case of the electron-impact-excited (and ion-impact-excited) electron emission spectra: (i) the well grounded Eu foil was presumed to be uncharged since no suitable reference peak was available; (ii) the $EuAl_2$ surface potential was monitored using the Al $L_{23}VV$ peak at 64.0 eV [51], but no charging was detected; and (iii) the Eu_2O_3 surface charge, typically −5 eV, was measured using the O $KL_{23}L_{23}$ Auger peak at 508.0 eV (as determined from the x-ray-excited spectrum).

3. Results

3.1. Electron-impact-excited spectra of Eu, $EuAl_2$ and Eu_2O_3

Electron emission spectra (50–550 eV) recorded from ion-sputter-etched samples of Eu metal, $EuAl_2$ and Eu_2O_3 are displayed in figure 1. These spectra were excited by 3 keV electron impact using 2–5 nA of beam current; the data were collected in the pulse-counting mode and subsequently differentiated and smoothed numerically. The spectra of Eu and Eu_2O_3 are consistent with clean surfaces, whilst the spectrum of $EuAl_2$ reveals minor levels of surface contamination (carbon and oxygen). Between 70 and 150 eV there is a complex emission structure, in all three spectra, which arises from excitation of the europium 4d subshell. A minor peak near 230 eV, which is most apparent in the Eu metal spectrum, has been assigned to europium 4p-based Auger transitions ($N_3O_{23}N_{67}$ and $N_3O_{23}V$) [1]. The $EuAl_2$ spectrum also has a strong peak, at 67 eV (maximum negative excursion), due to the $L_{23}VV$ Auger transition of aluminium [51].

The 4d-based electron emission structure of europium, excited by 3 keV electron impact, is shown in the $N(E)E$ format in figure 2. A linear background, with a negative slope, has been subtracted from the Eu_2O_3 spectrum. The spectra of Eu, $EuAl_2$ and Eu_2O_3 are similar; in each case, there are four prominent electron emission peaks, near 80, 100, 120 and 133 eV, which can be attributed mainly to the $N_{45}O_{23}O_{23}$, $N_{45}O_{23}N_{67}$, $N_{45}N_{67}N_{67}$ and 4f(4d ← 4f) transitions, respectively [1]. Significant differences, however, are also apparent between these spectra. The three most intense peaks for Eu_2O_3 are shifted towards lower kinetic energies, by 1–2 eV, relative to the corresponding peaks in the two other spectra. A minor emission feature is evident near 128 eV in the Eu and $EuAl_2$ spectra. The most intense peak, near 100 eV, is roughly symmetric for $EuAl_2$ and Eu_2O_3, but it has a pronounced shoulder on the low-kinetic-energy side for Eu.

Figures 3, 4 and 5 show the 4d-based electron emission structure of Eu, $EuAl_2$ and Eu_2O_3, respectively, for a wide range of primary electron-impact energies E_p. A linear background has been subtracted from most of these spectra; for Eu and $EuAl_2$ the background has an increasingly positive slope with decreasing E_p (negligible at 5 keV), whereas for Eu_2O_3 it changes from a negative slope (E_p = 3 or 2 keV) to a positive one (E_p = 500 eV). The spectrum obtained for Eu metal at E_p = 2 keV agrees well with a Eu spectrum published by Rivière *et al* (E_p = 1.6–2 keV) [1], when allowance is made for the difference in electron kinetic energy referencing (vacuum versus Fermi level). Significant changes are observed in the emission structure between 110 and 130 eV for

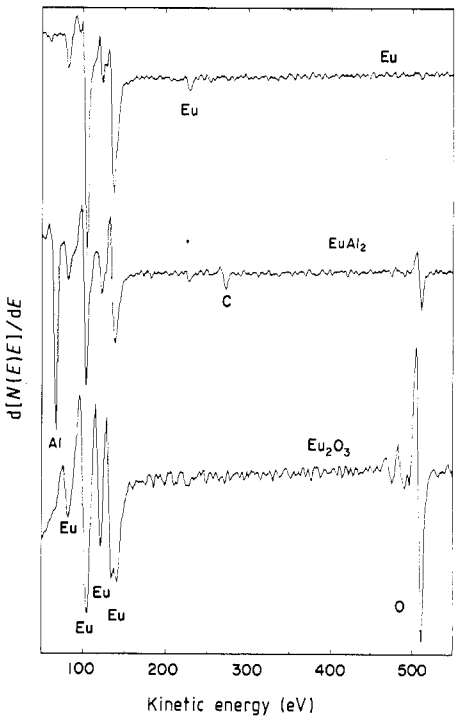

Figure 1. Electron emission survey spectra excited from ion-sputter-etched samples of Eu metal, $EuAl_2$ and Eu_2O_3 by 3 keV electron impact. The data were collected in the pulse-counting mode and subsequently differentiated and smoothed numerically.

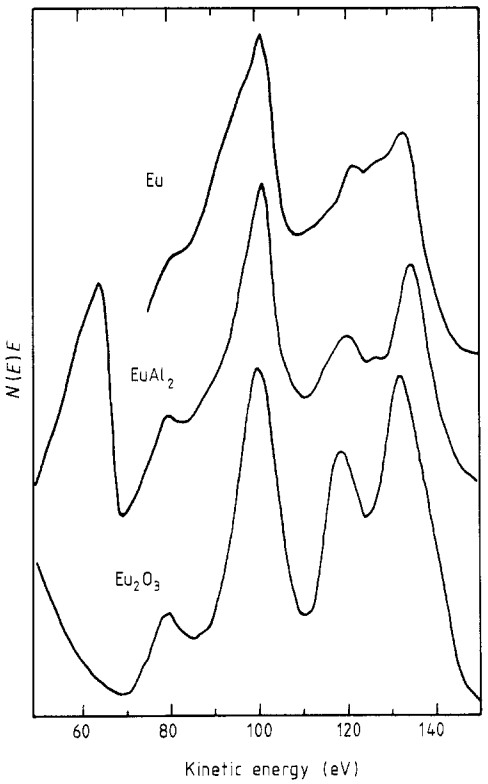

Figure 2. The 4d-based electron emission structure of europium, excited by 3 keV electron impact from Eu metal, $EuAl_2$ and Eu_2O_3. A linear background, with a negative slope, has been subtracted from the Eu_2O_3 spectrum.

Eu metal (figure 3) as E_p is decreased from 5 keV to 500 eV. Aside from the dominant peak at 121 eV, there appear to be at least two, and possibly three, minor emission features in this region, whose relative intensities depend strongly on the primary electron energy. Furthermore, the shoulder on the low-kinetic-energy side of the intense 101 eV peak is partly suppressed at low E_p, permitting the 80 eV peak to be more clearly resolved. Similar but less pronounced changes are observed in the electron emission structure of $EuAl_2$ as E_p is varied. The electron emission spectra of Eu_2O_3, however, do not provide any clear evidence of additional minor peaks. For all three materials, the strong peak near 133 eV gains intensity relative to the other major peaks with decreasing primary electron energy.

Electron energy loss spectra of Eu, $EuAl_2$ and Eu_2O_3, showing the europium giant resonance excitation, $[Kr]4d^{10}5s^25p^64f^nV^{n^*} \rightarrow [Kr]4d^95s^25p^64f^nV^{n^*}\,\overline{4,\varepsilon f}^1$, are displayed in figure 6. These spectra were recorded in the $N(E)E$ mode using reflection geometry with $E_p = 500$ eV and a linear background was subtracted from each raw data set to emphasise the core-excitation peaks. For Eu and $EuAl_2$, a single major electron energy loss feature, with the peak maximum near 140.5 eV (loss energy), has been

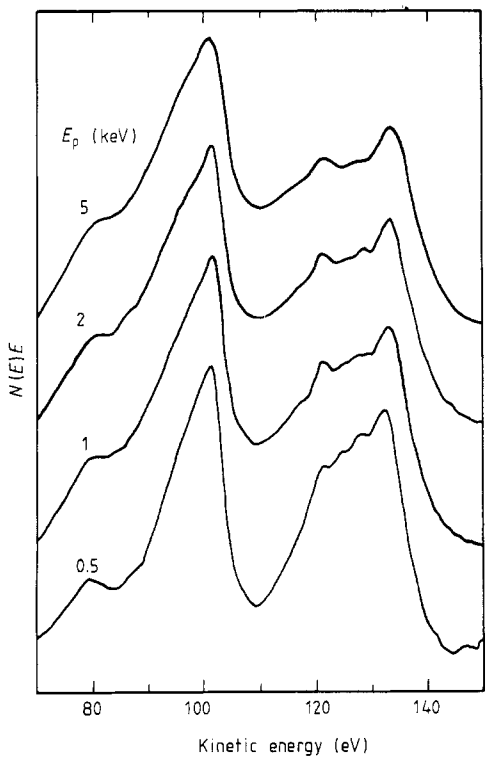

Figure 3. The 4d-based electron emission structure of Eu metal as a function of primary electron-impact energy. A linear background with a positive slope has been subtracted from the spectra excited with $E_p \leq 2$ keV.

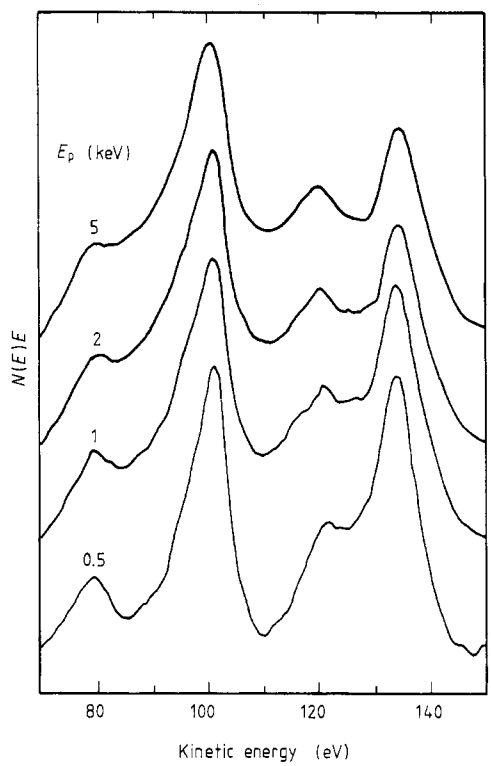

Figure 4. The 4d-based electron emission structure of $EuAl_2$ as a function of primary electron-impact energy. A linear background with a positive slope has been subtracted from the spectra excited with $E_p \leq 2$ keV.

observed. The Eu loss feature, however, is considerably broader and less symmetric than the $EuAl_2$ loss peak. A qualitatively different loss structure has been recorded for Eu_2O_3: an asymmetric doublet with the more intense component at 143.0 eV. All three spectra show evidence of minor peaks at lower loss energies. Felton *et al* [7] and Strasser *et al* [40] have published electron energy loss spectra for clean europium and oxygen-exposed europium that agree well with the spectra of Eu metal and Eu_2O_3, respectively, displayed in figure 6. The 2.5 eV shift in the position of the main loss peak, which is observed when the number of 4f electrons changes from seven (Eu and $EuAl_2$) to six (Eu_2O_3), provides a signature of the europium oxidation state [38].

3.2. X-ray-excited spectra of Eu, $EuAl_2$ and Eu_2O_3

The 4d-based electron emission spectra excited from Eu, $EuAl_2$ and Eu_2O_3 by Al Kα x-radiation are displayed in figure 7. These data were collected in the pulse-counting mode and numerically smoothed but not background subtracted. The three spectra are quite similar, although subtle differences in peak shapes and relative intensities are also evident. Each spectrum consists of a strong asymmetric doublet, with peaks at 97 and 116 eV, plus a weaker feature just below 80 eV. A minor shoulder near 133 eV in the

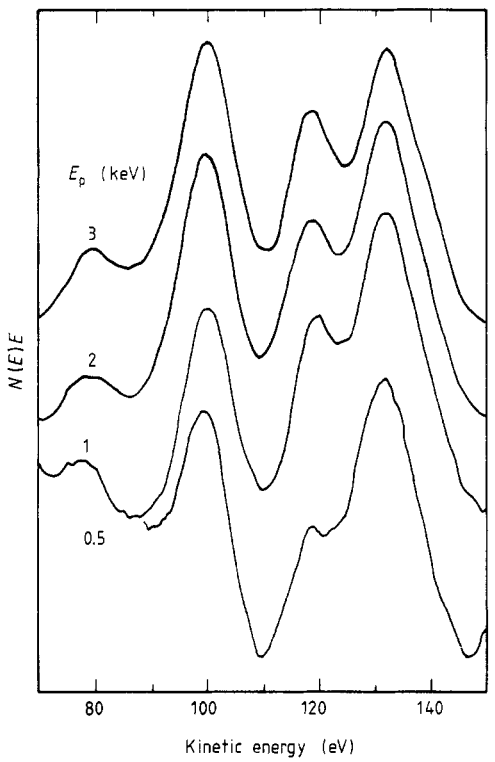

Figure 5. The 4d-based electron emission structure of Eu_2O_3 as a function of primary electron-impact energy. A linear background, with a negative slope for $E_p = 2$ and 3 keV and a positive slope for $E_p = 0.5$ keV, has been subtracted from these spectra.

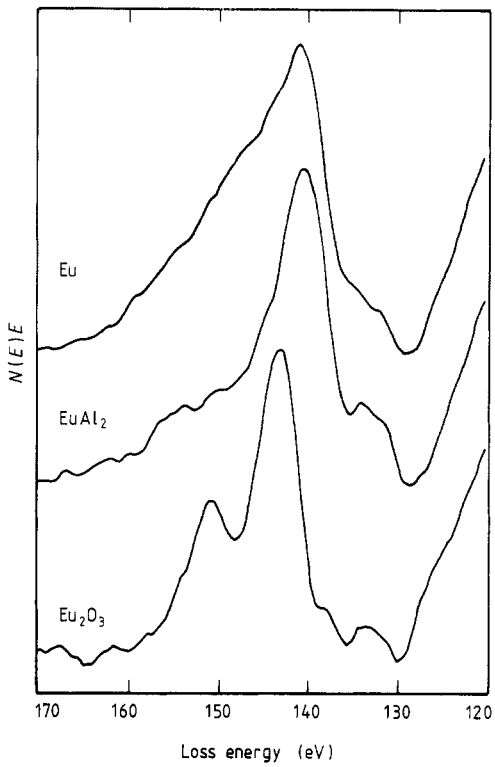

Figure 6. Electron energy loss spectra of Eu metal, $EuAl_2$ and Eu_2O_3 showing the europium 4d → 4f giant resonance excitation. The spectra were recorded using reflection geometry and a linear background was subtracted from each data set. E_p = 500 eV.

Eu and $EuAl_2$ spectra presumably arises from indirect excitation of the 4f(4d ← 4f) emission. The absence of an Al $L_{23}VV$ peak from the $EuAl_2$ spectrum is consistent with the low photoionisation cross section for the Al 2p subshell with Al Kα x-radiation (σ(Eu 4d)/σ(Al 2p) ≃ 18) [52]. Instead, a small dip in electron emission is seen near 68 eV (about 73 eV relative to the Fermi level). This may be due to a disappearance-potential effect in which electrons leaving the solid are preferentially removed from the background at energies above the Al 2p threshold [53–55].

Figures 8–10 present a detailed comparison of the influence of x-ray excitation versus electron-impact excitation on the 4d-based electron emission structure of europium. For Eu metal, the very weak shoulder on the high-kinetic-energy side of the x-ray-excited emission is well aligned with the direct recombination peak, at 133.2 eV, excited by electron impact. The two remaining major peaks in the x-ray-excited spectrum of Eu metal, however, are shifted, by about 5 eV, towards lower kinetic energies relative to the corresponding emission peaks in the electron-impact-excited spectrum. A similar behaviour has been observed for $EuAl_2$: alignment of the residual and intense direct recombination features, but a shift of the two major peaks in the Al Kα excited spectrum towards lower kinetic energies, by about 4 eV. The x-ray-excited spectrum of Eu_2O_3

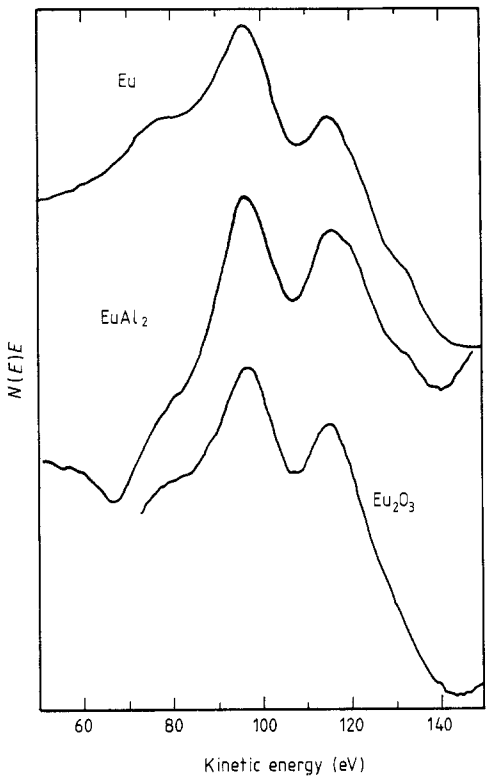

Figure 7. 4d-based electron emission spectra excited from ion-sputter-etched samples of Eu metal, $EuAl_2$ and Eu_2O_3 by Al Kα x-radiation.

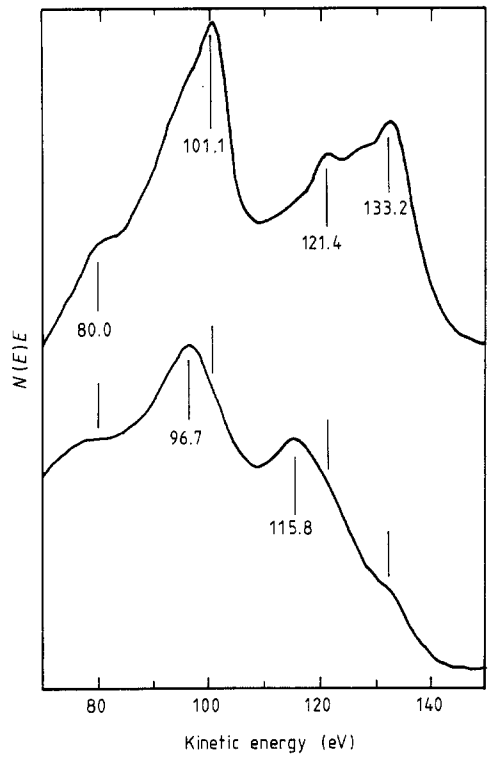

Figure 8. Comparison of the 4d-based electron emission spectra excited from Eu metal by 3 keV electron impact (upper trace) and Al Kα x-radiation (lower trace).

shows no evidence of a residual direct recombination feature, whilst the two remaining major peaks are again shifted, by about 3 eV, towards lower kinetic energies.

3.3. Ion-impact-excited spectrum of Eu

The 4d-based electron emission spectrum excited from Eu metal by 4.5 keV Ar^+ bombardment is shown in figure 11; a linear background has been subtracted from the smoothed $N(E)E$ data. No additional structure was evident within the kinetic energy range 20–1000 eV. The displayed spectrum consists of a broad asymmetric doublet with a pronounced shoulder on the low-energy side. It is similar in appearance to the corresponding spectrum excited by Al Kα x-radiation; in particular, there is little indication of 4f(4d $\leftarrow$ 4f) emission. Conversely, the peak kinetic energies are in good agreement (about 1 eV) with the Eu 4d-based Auger transitions excited by electron impact. At a more glancing angle of ion incidence (52° rather than 33° from the surface normal) the electron emission structure seen in figure 11 was hardly discernible above a smooth background.

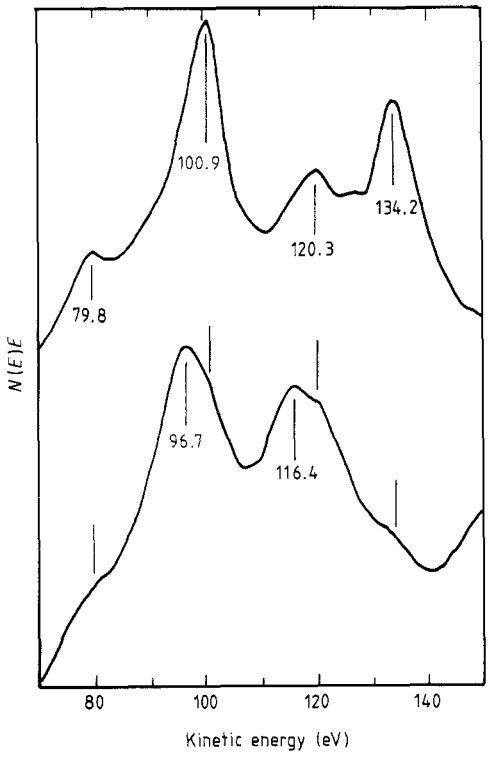

Figure 9. Comparison of the 4d-based electron emission spectra excited from $EuAl_2$ by 3 keV electron impact (upper trace) and Al Kα x-radiation (lower trace).

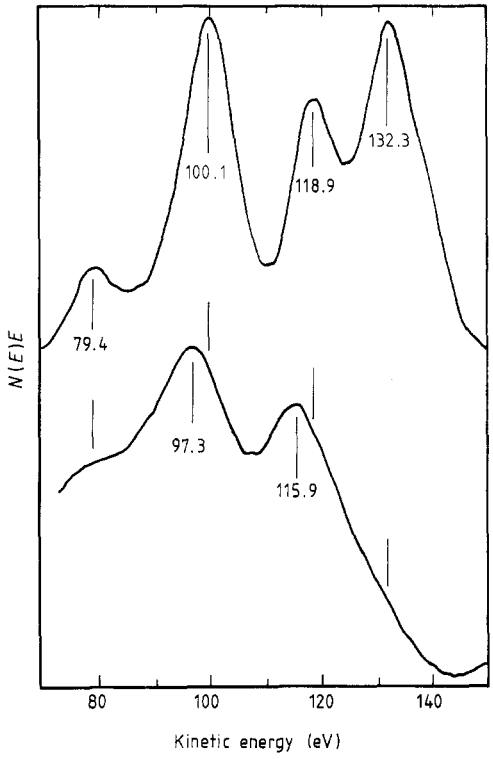

Figure 10. Comparison of the 4d-based electron emission spectra excited from Eu_2O_3 by 3 keV electron impact (upper trace) and Al Kα x-radiation (lower trace).

4. Discussion

The kinetic energy E_{DR} of the electron emission that arises from a direct recombination transition may be determined from the corresponding giant resonance excitation energy E_{GR} using the expression [1, 26, 56]

$$E_{DR} = E_{GR} - W_Y - \varphi_{sp} \tag{1}$$

where φ_{sp} is the spectrometer work function and W_Y is the binding energy of the electron ejected from level Y. Calculated values for the 4f(4d $\leftarrow$ 4f) and 5p(4d $\leftarrow$ 4f) direct recombination transition energies of Eu, $EuAl_2$ and Eu_2O_3 are collected in table 1. The position of the main peak in the electron energy loss spectrum was equated to E_{GR}, whilst the 4f and 5p binding energies were taken from XPS studies [1, 57–60]. A weighted average binding energy was used for the 5p level, which exhibits spin–orbit splitting of about 5 eV. Good agreement with experiment has been obtained for the 4f(4d $\leftarrow$ 4f) transition; however, the 5p(4d $\leftarrow$ 4f) transition does not appear to have greatly influenced the electron emission structure excited by electron impact, although there is evidence of a weak shoulder at the predicted energy in several spectra (see figures 3 and 4). This is consistent with the known relative 5p and 4f partial photoionisation cross sections ($I(4f) \simeq 10I(5p)$) for $h\nu = E_{GR}$ [1, 31].

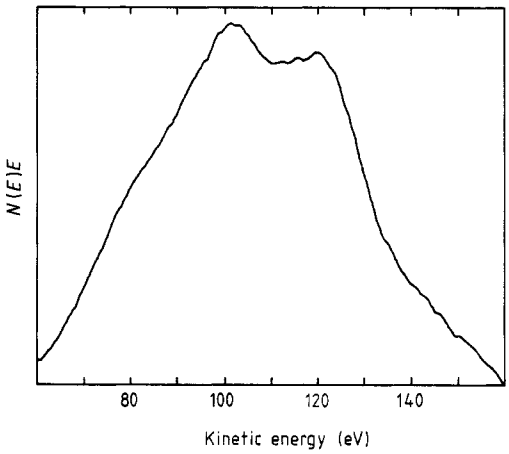

Figure 11. 4d-based electron emission spectrum of Eu metal excited by 4.5 keV Ar^+ bombardment. A linear background with a positive slope has been subtracted from the smoothed $N(E)E$ data.

Table 1. Direct recombination transition energies of europium. $\bar{W}_{5p}$ is the weighted average of the $5p_{1/2}$ and $5p_{3/2}$ binding energies. The experimental values are the observed peak positions for the 4f(4d ← 4f) direct recombination transition. W_{4f} for Eu, $EuAl_2$ and Eu_2O_3 and $\bar{W}_{5p}$ for Eu were taken from [1] and [57–60]; $\bar{W}_{5p}$ for $EuAl_2$ is an assumed value. $\bar{W}_{5p}$ for Eu_2O_3 is taken from this work.

	E_{GR} (eV)	W_{4f} (eV)	$\bar{W}_{5p}$ (eV)	Calculated E_{DR} (eV) 5p(4d ← 4f)	4f(4d ← 4f)	Experimental values (eV) 4f(4d ← 4f)
Eu	140.7	2.0	20.8	115.6	134.4	133.2
$EuAl_2$	140.5	1.0	(20.8)	115.4	135.2	134.2
Eu_2O_3	143.2	7.0	23.2	115.7	131.9	132.3

The weak features near 128 and 125 eV in the electron-impact-excited spectrum of Eu metal can be assigned to 4f(4d ← 4f) direct recombination processes arising from discrete 4d → 4f resonance excitations. A number of sharp resonances near or below the 4d ionisation threshold of europium have been identified as multiplet components of the $[Kr]4d^{10}5s^25p^64f^nV^{n^*} \rightarrow [Kr]4d^95s^25p^64f^nV^{n^*}\,\overline{4,\varepsilon}f^1$ transition [11, 12, 40]. The most intense discrete resonance peaks of Eu metal occur at 135 and 132 eV, in both photoabsorption and electron energy loss spectra [12, 19, 31, 40]. These excitations are predicted, using equation (1), to result in 4f(4d ← 4f) direct recombination emission at 129 and 126 eV, respectively, in good agreement with experiment. Furthermore, the 132 eV EELS peak gains intensity relative to other energy loss features at low electron-impact energy [40], consistent with the E_p dependence of the electron emission structure in figure 3 (the peak near 125 eV is clearly present only for $E_p = 500$ eV). Gerkin *et al* [26] have reported equivalent 4f(4d ← 4f) direct recombination assignments for gadolinium, which has the same configuration as Eu metal ($4f^7$) and a very similar electron emission spectrum [1].

Auger decay of core holes in the 4p subshell of europium should provide significant electron emission intensity between 70 and 150 eV [1, 61, 62]; however, it seems unlikely that $N_{23}N_{45}X$ (X ≡ V, N_{67}, O_{23}) Auger transitions substantially influence the electron

Table 2. Summary of 4d-based Auger transitions of europium. For Eu metal and $EuAl_2$, $n = 7$; for Eu_2O_3, $n = 6$.

Initial state	Final state		Designation
	Normal Auger transitions		
$[Kr]4d^9 5s^2 5p^6 4f^n V^{n*}$	$\rightarrow [Kr]4d^{10} 5s^2 5p^6 4f^{n-2} V^{n*}$	+ e	$N_{45}N_{67}N_{67}$
	$\rightarrow [Kr]4d^{10} 5s^2 5p^5 4f^{n-1} V^{n*}$	+ e	$N_{45}O_{23}N_{67}$
	$\rightarrow [Kr]4d^{10} 5s^2 5p^4 4f^n V^{n*}$	+ e	$N_{45}O_{23}O_{23}$
	$\rightarrow [Kr]4d^{10} 5s^2 5p^6 4f^{n-1} V^{n*-1}$	+ e	$N_{45}N_{67}V$
	$\rightarrow \ldots$		
	Auger transitions with a spectator electron		
$[Kr]4d^9 5s^2 5p^6 4f^n V^{n*} \overline{4, \varepsilon f}^1$	$\rightarrow [Kr]4d^{10} 5s^2 5p^6 4f^{n-2} V^{n*} \overline{4, \varepsilon f}^1$	+ e	$N_{45}N_{67}N_{67}(\overline{4, \varepsilon f})$
	$\rightarrow [Kr]4d^{10} 5s^2 5p^5 4f^{n-1} V^{n*} \overline{4, \varepsilon f}^1$	+ e	$N_{45}O_{23}N_{67}(\overline{4, \varepsilon f})$
	$\rightarrow [Kr]4d^{10} 5s^2 5p^4 4f^n V^{n*} \overline{4, \varepsilon f}^1$	+ e	$N_{45}O_{23}O_{23}(\overline{4, \varepsilon f})$
	$\rightarrow \ldots$		
	Auger transitions with a spectator vacancy		
$[Kr]4d^8 5s^2 5p^6 4f^n V^{n*}$	$\rightarrow [Kr]4d^9 5s^2 5p^6 4f^{n-2} V^{n*}$	+ e	$N_{45}N_{45}$–$N_{45}N_{67}N_{67}$
	$\rightarrow [Kr]4d^9 5s^2 5p^5 4f^{n-1} V^{n*}$	+ e	$N_{45}N_{45}$–$N_{45}O_{23}N_{67}$
	$\rightarrow [Kr]4d^9 5s^2 5p^4 4f^n V^{n*}$	+ e	$N_{45}N_{45}$–$N_{45}O_{23}O_{23}$
	$\rightarrow \ldots$		
$[Kr]4d^9 5s^2 5p^6 4f^{n-1} V^{n*}$	$\rightarrow [Kr]4d^{10} 5s^2 5p^6 4f^{n-3} V^{n*}$	+ e	$N_{45}N_{67}$–$N_{67}N_{67}N_{67}$
	$\rightarrow [Kr]4d^{10} 5s^2 5p^5 4f^{n-2} V^{n*}$	+ e	$N_{45}N_{67}$–$N_{67}O_{23}N_{67}$
	$\rightarrow [Kr]4d^{10} 5s^2 5p^4 4f^{n-1} V^{n*}$	+ e	$N_{45}N_{67}$–$N_{67}O_{23}O_{23}$
	$\rightarrow \ldots$		

emission peak positions observed in this region with either excitation mode. For electron-impact excitation, Rivière *et al* [1] have estimated that the probability of 4p ionisation is approximately a quarter of the probability of 4d ionisation. They also suggested that $N_{23}N_{45}X$ transitions merely contribute to the underlying electron emission intensity, owing to a wide range of final-state multiplet energies and large core-hole broadening. For Al Kα x-radiation, calculated photoionisation cross sections indicate that the probability of 4d ionisation is about twice the probability of 4p ionisation [52], whilst the experimental XPS peak intensity ratio appears to be even larger (4d to 4p ratio, about 3). Furthermore, the $N_3O_{23}N_{67}$ peak is very weak with both excitation modes; it is clearly detected only for Eu metal and is more than an order of magnitude less intense than the corresponding 4d-based feature.

The prominent features between 75 and 125 eV in the electron emission spectra of Eu, $EuAl_2$ and Eu_2O_3 are thus presumably due to 4d-based Auger transitions. Depending upon the nature of the excitation, however, three distinct classes of Auger transitions are feasible, as summarised in table 2. Normal Auger transitions are initiated by ionisation of a single 4d electron, without direct participation of the remaining electrons; the final-state ion then has two outer-shell holes that are screened only by relaxation processes [63, 64]. Auger electron emission following 4d $\rightarrow$ 4f giant resonance excitation occurs in the presence of a $\overline{4, \varepsilon f}$ spectator electron, which should provide enhanced screening in the final-state ion [18, 56, 64–66]. The complementary process, Auger electron emission with a spectator vacancy, requires a double-hole initial state [64]. Simultaneous ionisation of a second electron during creation of a 4d vacancy is possible,

but it is unlikely to occur with a high probability [64]. Efficient production of europium ions with two inner-shell vacancies could be achieved, however, by a sequential process involving deep inner-shell ionisation (e.g. 3d) followed by normal Auger transitions (e.g. $M_{45}N_{45}N_{45}$).

The kinetic energy $E(ABC)$ of the electron emitted during a normal Auger transition may be expressed as a function of the binding energies W_i of the three levels involved in the process and the effective Coulomb interaction U_{eff} between the final-state holes using the relation [1, 63, 67]

$$E(ABC) = W_A - W_B - W_C - U_{eff} - \varphi_{sp}. \tag{2}$$

For the 4d-based transitions of europium, U_{eff} is difficult to estimate accurately and spin–orbit splitting and multiplet structure introduce further uncertainty. Rivière *et al* [1] have calculated approximate Auger peak positions for Eu metal using weighted average XPS binding energies and plausible U_{eff}-values; the key results (adjusted to a vacuum level reference) are as follows: $N_{45}O_{23}O_{23}$, 79 eV; $N_{45}O_{23}N_{67}$, 102 eV; $N_{45}N_{67}N_{67}$, 120 eV. Auger transitions involving the 5s and/or valence levels ($N_{45}O_1N_{67}$, $N_{45}O_1V$, $N_{45}O_{23}V$, $N_{45}N_{67}V$ and $N_{45}VV$) should be of lower intensity and nearly coincident with one of the three dominant transitions [1]. By employing a similar strategy (same U_{eff}-values), the principal 4d-based Auger electron peaks of Eu_2O_3 can be estimated to occur at 80, 101 and 118 eV. These predictions are in good agreement with the spectra excited by electron impact (both Eu and Eu_2O_3).

The presence of a $\overline{4, \varepsilon f}$ spectator electron should increase the kinetic energy of an ejected Auger electron by causing a substantial reduction in U_{eff} [64, 66]. A spin flip of one electron is required, during either the excitation or the Auger process, to reach the $[Kr]4d^{10}5s^25p^64f^{n-2}V^{n^*}\overline{4, \varepsilon f}^1$ final state for $n = 7$, because of the initial-state ^8S configuration (as classified in the *LS*-coupling limit) [1, 29]. Relative oscillator strengths calculated by Sugar [11] indicate that several important multiplet components of the $[Kr]4d^{10}5s^25p^64f^7V^{n^*} \xrightarrow{h\nu} [Kr]4d^95s^25p^64f^7V^{n^*}\overline{4, \varepsilon f}^1$ resonant photoabsorption transition involve a spin flip. Selection rules should be similar for electron-impact excitation with E_p well above threshold [40]. The other possible 4d-based Auger transitions of europium with a $\overline{4, \varepsilon f}$ spectator electron can all occur without any change in electron spin.

Satellite features in the resonant photoemission spectra of elemental gadolinium and europium have been assigned by Gerkin *et al* [29] to the $N_{45}N_{67}N_{67}(\overline{4, \varepsilon f})$ Auger transition. The maximum satellite emission intensity, however, was observed with the photon energy tuned to a discrete $4d \rightarrow 4f$ resonance line well below the main giant resonance excitation. Since the spin-flip multiplet components of the $4d \rightarrow 4f$ transition (for Gd and Eu) are all predicted to contribute to the main giant resonance feature (at a higher excitation energy) [11], the $[Kr]4d^{10}5s^25p^64f^5v^{n^*}\overline{4, \varepsilon f}^1$ final state may be accessible only via a spin flip during the decay process. This behaviour might be understandable within the context of the discussion by Becker *et al* [17] of orbital-collapse effects in resonant photoemission from atomic Eu. The main $4d \rightarrow 4f$ giant resonance excitation involves promoting a 4d electron into a hybrid $l = 3$ level with substantial continuum (εf) as well as localised (nf) character [11–17]; decay channels in which the $\overline{4, \varepsilon f}$ electron participates then naturally dominate those in which it remains as a spectator. Conversely, the multiplet components of the $4d \rightarrow 4f$ transition that give rise to discrete resonances near or below the 4d ionisation threshold may with greater probability lead to decay processes in which the excited $\overline{4, \varepsilon f}$ electron is a spectator, by virtue of being strongly localised in the inner well of the double-well potential [17]. The comparatively low

intensity of these discrete resonances, as observed by EELS or x-ray photoabsorption, then indicates that Auger transitions with a $\overline{4, \varepsilon f}$ spectator electron should make only a minor contribution to electron-impact-excited spectra of europium and gadolinium. Indeed, there is no obvious structure in the electron-impact-excited spectrum of Gd [1] corresponding to the $N_{45}N_{67}N_{67}(\overline{4, \varepsilon f})$ emission (kinetic energy of about 127–130 eV relative to the Fermi level) detected by resonant photoabsorption [29] (the resonant photoemission spectrum of Eu was not published). Spin-polarised electron emission spectroscopy on Eu and Gd, analogous to the work of Taborelli *et al* [44] but with (selective) resonant-photon rather than electron-impact excitation would be revealing.

The presence of a spectator vacancy should decrease the kinetic energy of an ejected Auger electron for localised final states [64]; however, it is difficult to predict the magnitude of this effect accurately. In x-ray-excited spectra of copper metal, an L_3M–$MM_{45}M_{45}$ satellite emission structure has been identified about 7 eV below the corresponding normal Auger transition [68, 69]. The role of Auger transitions with a spectator vacancy in 4d-based electron emission from europium depends greatly on the nature of the excitation. Under 0.5–5 keV electron bombardment, 4d ionisation should exceed the combined ionisation of all deeper subshells [1]. Conversely, with Al Kα x-radiation, the probability of deep inner-shell ionisation is greater than the probability of 4d ionisation by about an order of magnitude [52]. In particular, calculated photoionisation cross sections indicate sevenfold greater ionisation of the 3d subshell than the 4d subshell. Since the 3d core holes decay mainly by $M_{45}N_{45}N_{45}$ and $M_{45}N_{45}N_{67}$ Auger transitions [62, 70, 71], this provides an extremely efficient mechanism for producing double-hole ($4d^{-2}$ and $4d^{-1}4f^{-1}$) europium ions with at least one vacancy in the 4d subshell. Photoionisation of the $3p_{3/2}$, 4s and 4p subshells opens alternative secondary channels to appropriate double-hole initial states. The 4d-based satellite transitions of europium with one 4d or 4f spectator vacancy have been estimated to occur approximately 5 eV below the corresponding normal Auger transitions [72]. Channels involving triple-hole initial states are also possible, by sequential Auger transitions (e.g. $M_3M_5M_{67}$ plus M_5N_{67}–$N_{67}N_{45}N_{45}$, and $M_4M_5N_{67}$ plus M_5N_{67}–$N_{67}N_{45}N_{45}$), but should be less significant; they are likely to be still lower in energy and would cause broadening of the main satellite Auger peaks. Thus, Auger transitions with a spectator vacancy evidently dominate the 4d-based electron emission spectra excited from Eu, $EuAl_2$ and Eu_2O_3 by Al Kα x-radiation but have only a minor influence on their electron-impact-induced counterparts.

The above situation has similarities to, but also important differences from, the recently observed enhancement of the L_{23}^2–$L_{23}VV$ satellite structure in the electron emission spectrum of silicon excited by synchrotron radiation above the Si 1s threshold [73]. In both cases, the satellite structure (Auger emission with a spectator hole) arises predominantly by cascade from a deeper core level. For silicon, however, the fact that the final-state valence holes are delocalised has two significant consequences: (i) the satellite structure appears at *higher* kinetic energy than the main $L_{23}VV$ peak; and (ii) the L_{23}^2–$L_{23}VV$ transition leads in turn to enhancement of normal $L_{23}VV$ Auger emission by creating single 2p core holes. Because of this latter effect, the satellite processes can never dominate the conventional Auger channel for silicon, as they may in the 4d spectra of the rare earths, excited by x-radiation above the 3d threshold.

The 4d-based electron emission excited from Eu metal by Ar^+ bombardment must largely originate from europium ions that are still incorporated in the solid surface. Neither the angular dependence of the emission intensity nor the short lifetime of the 4d core hole (10^{-15} s or less) [74] are consistent with electron emission from sputtered

europium ions [75]. The observed electron emission structure, which agrees well in energy with corresponding features excited by electron impact, can be reasonably attributed to normal 4d-based Auger transitions, mainly $N_{45}O_{23}O_{23}$, $N_{45}O_{23}N_{67}$ and $N_{45}N_{67}N_{67}$, following ion-induced 4d ionisation. Some broadening of the emission structure is presumably caused by the strongly perturbed environment of the europium ions within the collision cascade. Evidently, the $4d \rightarrow 4f$ giant resonance transition has not been excited by Ar^+ impact, since there is no indication of $4f(4d \leftarrow 4f)$ direct recombination electron emission.

Overall the atomistic picture of Auger and direct recombination processes presented here is very successful in interpreting the 4d-based electron emission spectra of europium. However, the fact that the spin polarisation of the 4d-based electron emission from gadolinium is less than predicted by simple atomic theory [44] suggests that there is some greater subtlety in the problem yet to be revealed.

5. Conclusions

The electron emission structure arising from excitation of the 4d subshell of europium by electron impact may be attributed primarily to the $N_{45}O_{23}O_{23}$, $N_{45}O_{23}N_{67}$ and $N_{45}N_{67}N_{67}$ normal Auger transitions and the $4f(4d \leftarrow 4f)$ direct recombination process. Auger transitions with a $\overline{4, \varepsilon f}$ spectator electron and the $5p(4d \leftarrow 4f)$ direct recombination process appear to be of secondary importance. The 4d-based electron emission excited from europium by Al Kα x-radiation is predominantly due to Auger transitions with a spectator vacancy: $N_{45}N\text{–}NO_{23}O_{23}$, $N_{45}N\text{–}NO_{23}N_{67}$ and $N_{45}N\text{–}NN_{67}N_{67}$. In both cases, 4d-based Auger transitions involving valence or 5s electrons and 4p-based Auger transitions merely contribute to the underlying electron emission intensity. Argon-ion bombardment of europium excites normal 4d-based Auger electron emission but not direct recombination electron emission.

Acknowledgments

The authors would like to thank D G Watson and K D Bomben, Physical Electronics, for recording the x-ray-excited electron emission spectra.

References

[1] Rivière J C, Netzer F P, Rosina G, Strasser G and Matthew J A D 1985 *J. Electron. Spectrosc. Relat. Phenom.* **36** 331
[2] Netzer F P, Bertel E and Matthew J A D 1981 *J. Phys. C: Solid State Phys.* **14** 1891
[3] Matthew J A D, Strasser G and Netzer F P 1982 *J. Phys. C: Solid State Phys.* **15** L1019
[4] Bertel E, Strasser G, Netzer F P and Matthew J A D 1982 *Surf. Sci.* **118** 387
[5] Chorkendorff I, Onsgaard J, Aksela H and Aksela S 1983 *Phys. Rev.* B **27** 945
[6] Onsgaard J, Chorkendorff I and Sorensen O 1983 *Phys. Scr.* T **4** 169
[7] Felton R C, Prutton M, Matthew J A D and Zinn W 1979 *Surf. Sci.* **79** 117
[8] Dufour G, Karnatak R C, Mariot J M and Bonnelle C 1976 *J. Physique* **37** L119
[9] Dufour G and Bonnelle C 1974 *J. Physique* **35** L255
[10] Färber W and Braun P 1974 *Surf. Sci.* **41** 195
[11] Sugar J 1972 *Phys. Rev.* B **5** 1785
[12] Mansfield M W D and Connerade J P 1976 *Proc. R. Soc.* A **352** 125

[13] Connerade J P 1978 *Contemp. Phys.* **19** 415
[14] Connerade J P 1983 *J. Less-Common Met.* **93** 171
[15] Cheng K T and Fischer C F 1983 *Phys. Rev.* A **28** 2811
[16] Meyer M, Prescher Th, Raven E v, Richter M, Schmidt E, Sonntag B and Wetzel H E 1986 *Z. Phys.* D **2** 347
[17] Becker U, Kerkhoff H G, Lindle D W, Kobrin P H, Ferrett T A, Heimann P A, Truesdale C M and Shirley D A 1986 *Phys. Rev.* A **34** 2858
[18] Netzer F P and Matthew J A D 1986 *Rep. Prog. Phys.* **49** 621
[19] Zimkina T M, Fomichev V A, Gribovskii S A and Zhukova I I 1967 *Sov. Phys.–Solid State* **9** 1128
[20] Fomichev V A, Zimkina T M, Gribovskii S A and Zhukova I I 1967 *Sov. Phys.–Solid State* **9** 1163
[21] Haensel R, Rabe P and Sonntag B 1970 *Solid State Commun.* **8** 1845
[22] Aono M, Chiang T C, Himpsel F J and Eastman D E 1981 *Solid State Commun.* **37** 471
[23] Gudat W, Alvarado S F and Campagna M 1978 *Solid State Commun.* **28** 943
[24] Allen J W, Johansson L I, Bauer R S, Lindau I and Hagström S B M 1978 *Phys. Rev. Lett.* **41** 1499
[25] Johansson L I, Allen J W, Gustafsson T, Lindau I and Hagström S B M 1978 *Solid State Commun.* **28** 53
[26] Gerken F, Barth J, Kobayashi K L I and Kunz C 1980 *Solid State Commun.* **35** 179
[27] Aono M, Chiang T C, Knapp J A, Tanaka T and Eastman D E 1980 *Phys. Rev.* B **21** 2661
[28] Allen J W, Johansson L I, Lindau I and Hagström S B 1980 *Phys. Rev.* B **21** 1335
[29] Gerken F, Barth J and Kunz C 1981 *Phys. Rev. Lett.* **47** 993
[30] Egelhoff W F, Tibbetts G G, Hecht M H and Lindau I 1981 *Phys. Rev. Lett.* **46** 1071
[31] Gerken F, Barth J and Kunz C 1982 *X-ray and Atomic Inner Shell Physics (AIP Conf. Proc. 94)* ed B Crasemann (New York: American Institute of Physics) p 602
[32] Barth J, Gerken F, Schmidt-May J, Flodstrom A and Johansson L I 1983 *Chem. Phys. Lett.* **96** 532
[33] Schmidt-May J, Gerken F, Nyholm R and Davis L C 1984 *Phys. Rev.* B **30** 5560
[34] Trebbia P and Colliex C 1973 *Phys. Status Solidi* b **58** 523
[35] Nigavekar A and Matthew J A D 1980 *Surf. Sci.* **95** 207
[36] Bertel E, Netzer F P and Matthew J A D 1981 *Surf. Sci.* **103** 1
[37] Strasser G, Bertel E, Matthew J A D and Netzer F P 1982 *Valence Instabilities* ed P Wachter and H Boppart (Amsterdam: North-Holland) p 169
[38] Netzer F P, Strasser G and Matthew J A D 1983 *Solid State Commun.* **45** 171
[39] Netzer F P, Strasser G and Matthew J A D 1983 *Phys. Rev. Lett.* **51** 211
[40] Strasser G, Rosina G, Matthew J A D and Netzer F P 1985 *J. Phys. F: Met. Phys.* **15** 739
[41] Richter M, Prescher T, Meyer M, Raven E v, Sonntag B, Wetzel H E and Aksela S 1988 *Phys. Rev.* B **38** 1763
[42] Dzionk Ch, Fiedler W, Lucke M v and Zimmerman P 1989 *Phys. Rev. Lett.* **62** 878
[43] Zangwill A and Soven P 1980 *Phys. Rev.* A **21** 1561
[44] Taborelli M, Allenspach R and Landolt M 1986 *Phys. Rev.* B **34** 6112
[45] Connerade J P, Esteva J M and Karnatak R C (ed) 1987 *Giant Resonances in Atoms, Molecules and Solids* (New York: Plenum)
[46] Hocking W H, Tait J C and Hayward P J 1988 *Appl. Surf. Sci.* **32** 193
[47] Anthony M T *Practical Surface Analysis by Auger and X-Ray Photoelectron Spectroscopy* ed D Briggs and M P Seah (Chichester, West Sussex: Wiley) appendix 1
Wagner C D *Practical Surface Analysis by Auger and X-Ray Photoelectron Spectroscopy* ed D Briggs and M P Seah (Chichester, West Sussex: Wiley) appendix 4
[48] Schneider W D, Laubschat C, Nowik I and Kaindl G 1981 *Phys. Rev.* B **24** 5422
[49] Fadley C S, Hagström S B M, Klein M P and Shirley D A 1968 *J. Chem. Phys.* **48** 3779
[50] Uwamino Y, Ishizuka T and Yamatera H 1984 *J. Electron. Spectrosc. Relat. Phenom.* **34** 67
[51] Madden H H and Goodman D W 1985 *Surf. Sci.* **150** 39
[52] Scofield J H 1976 *J. Electron. Spectrosc. Relat. Phenom.* **8** 129
[53] Matthew J A D, Strasser G and Netzer F P 1984 *Phys. Rev.* B **30** 4975
[54] Nilsson P O and Kanski J 1973 *Surf. Sci.* **37** 700
[55] Taylor J A 1982 *J. Vac. Sci. Technol.* **20** 751
[56] Matthew J A D and Girvin S M 1981 *Phys. Rev.* B **24** 2249
[57] Lang J K, Baer Y and Cox P A 1981 *J. Phys. F: Met. Phys.* **11** 121
[58] Murgai V, Gupta L C, Parks R D, Martensson N and Reihl B 1982 *Valence Instabilities* ed P Wachter and H Boppart (Amsterdam: North-Holland) p 299
[59] Martensson N, Hillebrecht F U and Sarma D D 1985 *Surf. Sci.* **152–3** 733
[60] Laubschat C, Kaindl G, Schneider W D, Reihl B and Martensson N 1986 *Phys. Rev.* B **33** 6675

[61] McGuire E J 1975 *Sandia Laboratory Report* SAND-75-0443
[62] Coghlan W A and Clausing R E 1973 *At. Data* **5** 317
[63] Rivière J C 1985 *Theory and Applications of Auger Spectroscopy* ed G C Allen (Montreal: Multiscience) ch 1
[64] Thompson M, Baker M D, Christie A and Tyson J F 1985 *Auger Electron Spectroscopy (Chemical Analysis* vol 74) ed P J Elving, J D Winefordner and I M Kolthoff (New York: Wiley)
[65] Ramsey M G and Russell G J 1985 *Appl. Surf. Sci.* **22–3** 206
[66] Ramsey M G and Russell G J 1985 *Phys. Rev.* B **32** 3654
[67] McGuire G E and Holloway P H 1981 *Electron Spectroscopy: Theory, Techniques and Applications* vol 4, ed C R Brundle and A D Baker (London: Academic) ch 1
[68] Roberts E D, Weightman P and Johnson C E 1975 *J. Phys. C: Solid State Phys.* **8** L301
[69] Weightman P and Andrews P T 1979 *J. Phys. C: Solid State Phys.* **12** 943
[70] McGuire E J 1972 *Phys. Rev.* A **5** 1052
[71] Davis L E, MacDonald N C, Palmberg P W, Riach G E and Weber R E 1978 *Handbook of Auger Electron Spectroscopy* 2nd edn (Eden Prairie, MN: Perkin–Elmer Corporation)
[72] Hocking W H and Matthew J A D 1988 *J. Phys. C: Solid State Phys.* **21** L403
[73] Woicik J C, Pianetta P, Sorensen S L and Crasemann B 1989 *Phys. Rev.* B **39** 6048
[74] Fuggle J C and Alvardo S F 1980 *Phys. Rev.* A **22** 1615
[75] Matthew J A D 1983 *Phys. Scr.* T **6** 79